RUNNING STABILITY OF TRAIN ON VIBRATING TRACK SUBJECTED TO HORIZONTAL EXCITATION

N. Akiyama (1)
H. Kawakami (2)
Presenting Author: N. Akiyama

SUMMARY

In Honshu-Shikoku Bridge project, huge suspension bridges will be constructed as combination bridges of highway and railway. This study is mainly concerned with clarifying the safety-margin of railway vehicles from the lift-off up to critical states under horizontal excitations. 1/5-model vehicles are successfully employed to set up the suitable mechanical model describing rocking motions and 1/10-models for experimental verifications of the above margin. Temporarily increased amplitudes and extended frequencies in the transition from rolling to rocking are observed, that might cause crucial effects on the running stability. These phenomena are definitely confirmed by the proposed model.

INTRODUCTION

In Honshu-Shikoku Bridge project, five huge suspension bridges including the longest one in the world will be constructed as combination bridges of highway and railway. In these bridges, stiffening truss girders with double deck will be employed. The highway is located on the upper deck and the lower deck is used for the railway(Fig.1).

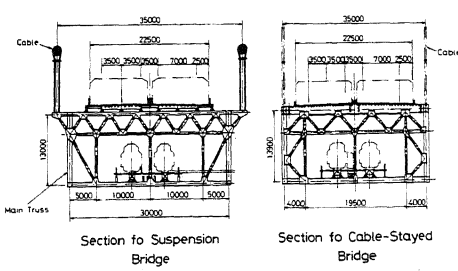

Fig.1

When a railway vehicle runs on a suspension bridge, its large flexibility sometimes put the vehicle to dangerous external forces due to winds, earthquakes, the vehicle itself and so on. Then the track is exposed to fierce excitations, and the conventional criteria on the stability of running vehicles would be misleading. The conventional criteria are exclusively concerned on the derailment in terms of the derailment coefficient Q/P(Q:side thrust,P:wheel load). The occurrence of derailment is governed by whether the derailment coefficient exceeds a certain critical value. Whenever either of wheels even slightly lifts off the rail, wheel load P_{ij} becomes null and the derailment coefficient turns into infinity. Nevertheless, lift-off does not always mean the immediate derailment.

(1) Professor of Structural Eng. Saitama University, Saitama, JAPAN

(2) Assistant of Structural Dynamics, Saitama University

In this connection, more than a decade, the extensive research works (Ref.1,2) have been conducted to make clear the reliable safety-margin from the lift-off through rocking up to derailment or overturning and the condition which governs these two critical phenomena. In the 1/5-model test, the emphasis is laid on setting-up the proper mechanical model which allows the quantitative explanation of test results. The 1/10-model test is mainly concerned with the experimental verification of the above safety-margin.

SIMILARITY LAW FOR MODEL TESTS

As gravity acceleration is intrinsic in dynamic tests, model-to-prototype acceleration ratio is put 1/1. We then choose the scale factor of length 1/5 and 1/10 (as large and small as possible) to preserve the rigorous similarity between models and prototypes, and to simulate as much as possible actual situations in prototypes, especially in suspension systems. The following similarity laws for 1/5- and 1/10-models are obtained:

	SCALE	FACTOR
Length	1/5	1/10
Acceleration	1/1	1/1
Mass	1/125	1/1000
Force	1/125	1/1000
Moment of inertia	1/325	1/100000
Time	$1/\sqrt{5}$	$1/\sqrt{10}$
Velocity	$1/\sqrt{5}$	$1/\sqrt{10}$
Frequency	$\sqrt{5}/1$	$\sqrt{10}/1$
Stiffness coefficient	1/25	1/100
Damping coefficient	$1/25\sqrt{5}$	$1/100\sqrt{10}$

Prototypes are WARA(2-axle with double linkage) and HOKI-300(2-axle bogie with TR-41 suspension) which are very popular freight cars in Japanese National Railway.

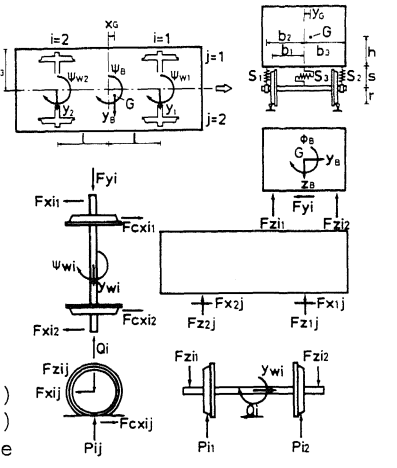

Fig.2 Mechanical Model of Running WARA-Type Vehicle

RUNNING TEST OF 1/5-MODEL

Proposed Mechanical Model for Running Condition and Equation of Motion

Fig.2 shows the proposed mechanical model of WARA-type vehicle. This model has 10 degrees of freedom, and enables us to set up the following equations of motion:

Car Body : $m_B\ddot{y}_B=-F_{y1}-F_{y2}$ $\quad m_B\ddot{z}_B=m_Bg-F_{z11}-F_{z12}-F_{z21}-F_{z22}$

$$I_{Bx}\ddot{\phi}_B=F_{z11}\{b_2+y_G+h\phi_B-(1-x_G)\psi_B\}-F_{z12}\{b_2-y_G-h\phi_B+(1-x_G)\psi_B\}$$
$$+F_{z21}\{b_2+y_G+h\phi_B+(1+x_G)\psi_B\}-F_{z22}\{b_2-y_G-h\phi_B-(1+x_G)\psi_B\}+F_{y1}h+F_{y2}h$$

$$I_{Bz}\ddot{\psi}_B=-F_{y1}(1-x_G)+F_{y2}(1+x_G)+F_{x11}\{b_2+y_G-(1-x_G)\psi_B\}$$
$$-F_{x12}\{b_2-y_G+(1-x_G)\psi_B\}+F_{x21}\{b_2+y_G+(1+x_G)\psi_B-F_{x22}\{b_2-y_G-(1+x_G)\psi_B\}$$

Wheelset : $m_W\ddot{y}_{Wi}=F_{yi}-Q_i \qquad I_{Wz}\ddot{\psi}_{Wi}=(F_{cxi1}-F_{cxi2})b_1-(F_{xi1}-F_{xi2})b_2$

$$I_{Wx}\ddot{\phi}_{Wi}=-F_{zi1}b_2+F_{zi2}b_2-P_{i2}+Q_ir+F_{yi}s$$

where
m_B, m_W : Masses of car body and wheelset
y_B, z_B ; y_W, z_W : Horizontal and vertical displacements of car body and wheelset, respectively
ϕ_B, ψ_B ; ϕ_W, ψ_W : Rolling and yawing angles of car body and wheelset, respectively
I_{Bx} : Moment of inertia of car body around x-axis
I_{Bz} : Moment of inertia of car body around z-axis
g : Gravity acceleration
x_G, y_G : Eccentricity of gravity center
$Q_i = F_{cyi1}+F_{cyi2}+(F_{cxi1}+F_{cxi2})\psi_{Wi}+F$
F_{cxij} , F_{cyij} : Creep forces along x-, y-axis, respectively
F_{Rij} : Reaction force of rail track upon wheel flange

The current theory replaces the running effects of a vehicle by creep forces which act on the vehicle through interfaces between wheels and rails. The linear creep theory is employed and creep coefficients along both x-and y-axis are assumed to be equal. This creep coefficient is calculated by Carter's formula(Ref.3) and Hertz's theory, and proportional to the 2/3 power of the wheel load(Ref.4).

On the Measured Spring Characteristics of 1/5-model (static and dynamic)

We come up with the mechanical model for WARA-type as follows:

(1) Car body and wheel set are rigid.
(2) Friction phenomena that might occur at linkage leaf-springs and wheel-rail interface are replaced by nonlinear springs.

The properties of these non-linear springs are determined by the static load-displacement curves which allow us to approximate by Bilinear or Trilinear curves. But in dynamic properties, the equivalent viscous damping is expected to play a vital role, so we must make clear the quantitative relationships between Coulomb and viscous dampings in oscillations. These dynamic

Fig.3 Hysteresis-Curve Variation by Excitation Acceleration

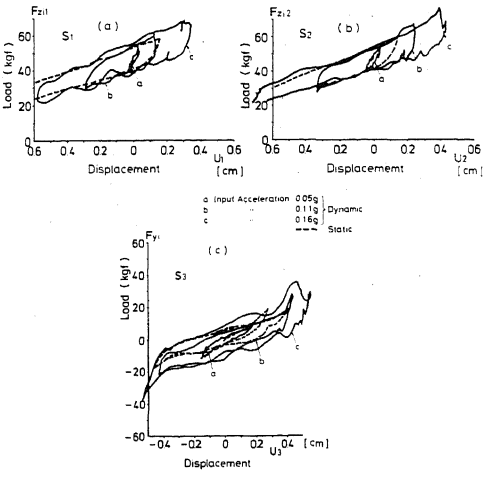

hysteresis curves are constructed from measured acceleration data of the six-degree-of freedom mechanical oscillator by double intergration. Typical hysteresis curves are given in Figs.3(a), (b) and (c). From these figures, it is possible that hysteresis curves for S_1 and S_2 are modelled by bilinear and for S_3 by trilinear curves, respectively. These figures show remarkable differences of the hysteresis loop between not only static and dynamic properties but also input accelerations. This implies the necessity of considering the effect of viscous damping.

Two-dimension Shaking Table and Measuring System

The set-up shaking table is composed of a box girder, 36 m long, 1.5 m wide, 0.65 m high and 18.5 t in weight. It can be accelerated sinusoidally by three actuators up to the max. horizontal displacement of 100 mm, the frequency of 10 Hz and the acceleration of 0.5 g. The box girder floats on its concrete slab foundation by means of a hydraulic servo-system through interchangeable springs. The track is installed on the shaking table, and this track is roughly divided into three portions; the acceleration portion, the test portion in the middle and the braking portion.

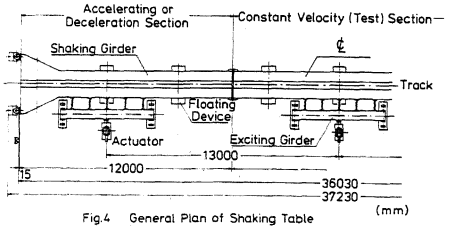

Fig.4 General Plan of Shaking Table

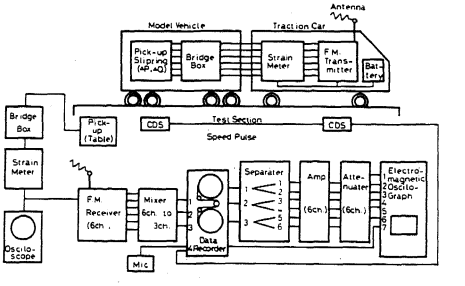

Fig.5 Measuring System (Ref.2)

Measuring system is schematized in Fig.5. Accelerations of the model vehicles are measured by the use of compact accelerometers. Strain meters, FM-transmitter and a battery for power supply are mounted on the traction car. Each signal from the accelerometers is first amplified by the strain meter on the traction car and transmitted to the FM-receiver on the ground by way of the FM-transmitter on the traction car. Wheel loads and side thrusts are measured by the use of wire strain gauges attached to the spoke wheel as shown in Fig.6. These informations are transmitted to the strain meter via slip-rings and then recorded in the data recorder in the same way as for the acceleration signals.

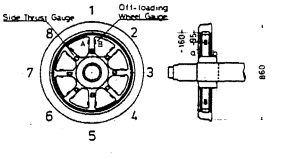

Strain Gauges Attachmnt to Spoke-Wheel (Ref.2)

Fig. 6

Comparison between Test and Numerical Analysis Results

Numerical calculations of response for WARA-type model are carried out by the mechanical model given in Fig.2. Input acceleration is given to the model from the rails through springs assuming that the left and right wheels are identically excited in the horizontal direction but

independently in the vertical direction. The hysteresis loops for S_1 and S_2 are improved by adding the tiny broken linear segments to the bilinear model(HEXA-model). Whenever either of wheel load $P_{i,j}$ assumes the negative value, which means the occurrence of lift-off, this value must be set equal to zero so that the proper calculation can proceed. Comparisons between test and numerical analysis results are given in Figs.7, in which $|\ddot{y}_R|$ and y_R denote the input (rail) acceleration, and the amplitude. These figures tell us that the excitation frequency 2.5 Hz is decisive for the two peculiar response spectra. For lower frequency, test values fall below calculated ones, while for higher frequency, the situation is reversed. On the whole, these comparisons show the fairly good agreement.

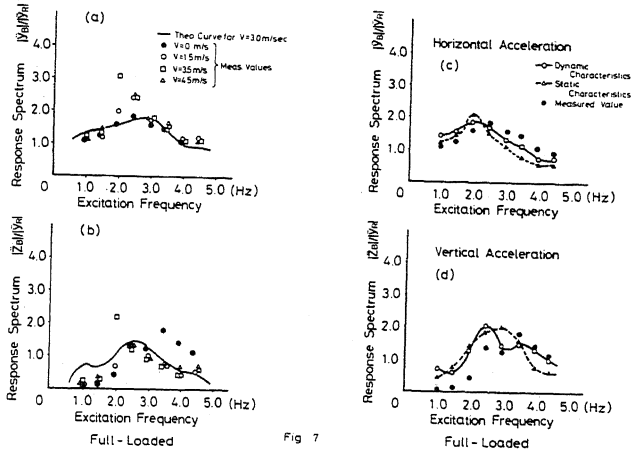

Fig 7

INTERRELATIONS BETWEEN OVERTURNING, ROCKING AND DERAILMENT (1/10-MODEL)

Introduction of 1/10-model

The weight of 1/5-model adds up to over 100 kg, and that makes it impossible to perform the test in critical states(overturning or derailment) from the safety viewpoint. The 1/10-model has 1/8 time that of 1/5-model, and rather simple and tiny safeguard systems are necessary for critical states. Objectives of 1/10-model test are summarized as follows:

(1) To narrow down the lift-off limit;
(2) To make clear how the critical states come out;
(3) To go over the process up to the critical states; and
(4) To establish interrelations between lift-off limit, overturning and derailment.

The Effect of Running Velocity upon the Critical Acceleration

The effect of the running velocity on the critical acceleration amplitude from rolling to rocking or vice versa are examined by choosing the excitation frequency of 2 Hz, where the rocking motion is pronounced. The standing car is subjected to the input acceleration just below the critical one. This acceleration amplitude is gradually increased, keeping a certain specified velocity of the model(0~ 1.1m/sec) up to the one when rocking motion starts, or vice versa. Test results are given in Figs.8(a), (b). These figures tell us that running velocity has almost nothing to do

with the critical acceleration amplitude, to be more precisely, the effect of running velocity stays within less than 5% in terms of standard deviation.

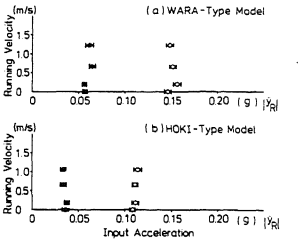

Fig. 8

Jumping Phenomena between Rolling and Rocking

In the 1/10-model test, overturning or derailment phenomena are, on some occaision, observed within the duration of several waves after rolling goes into rocking, and the car body violently oscillates immediately after rocking take place, on other occaision(Fig.9). In order to give the quantitative explanation to these phenomena, the car body measurements are made through the transition from rolling to rocking, or vice versa. The frequency of 3 Hz is chosen, and gradually increased the input acceleration amplitude. Fig.10 shows the acceleration, velocity and displacement waves, respectively. Rocking starts at the moment 4.6 sec and the transition continues up to the moment 6.0 sec after measurement is made. Afterwards, it has a stationary condition.

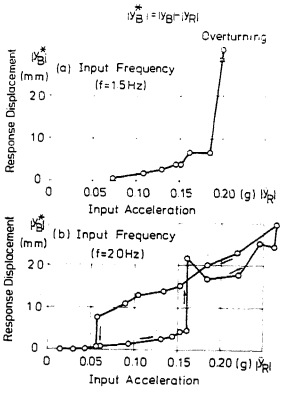

Fig. 9

In the horizontal acceleration of car body, the 15-Hz wave becomes noticeable with the input amplitude growth. This acceleration wave breaks into the two waves at crests, and one of them dominates to show the very distinguished form. During the transition to rocking, the wave temporarily shows the extended period and back to the original one (the input period) in the stationary rocking.

From figures of velocity waves, it is observed that the great changes in both wave forms and their amplitudes occur during and after the transition. These waves also show the temporarily extended period and larger amplitude during the transition.

Figures of the displacement waves tell that the amplitude input shows the slight and gradual increase up to the moment when rocking starts, and afterwards the input wave keeps the stationary condition. The horizontal displacement of the car body shows the abrupt change up to 1.6 times that of rolling at some point during the transition. This explains why the car body violently oscillates shortly after rocking starts.

Under some different condition, this is supposed to be followed by overturning or derailment. But as far as this test is concerned, the car

body shows the stationary rocking. Examination of phase lag from the input wave reveals that the horizontal displacement has the phase lag of about 35; while , in rocking this phase lag comes to about 140. In the rolling angle , the phase lag of -100° in rolling turns into that of -25° in rocking.

The following qualitative explanation can be given to these phenomena. Between rolling and rocking, complex frequency response functions are not the same, and these differences cause some changes not only in amplitudes but in phase lags. During the transition, some temporarily extended period is indispensable to connect the rolling with the rocking without interruption. This extended period is inevitably accompanied by the increased amplitude. These observed phenomena can be confirmed by the calculation using the present mechanical model in the large oscillation.

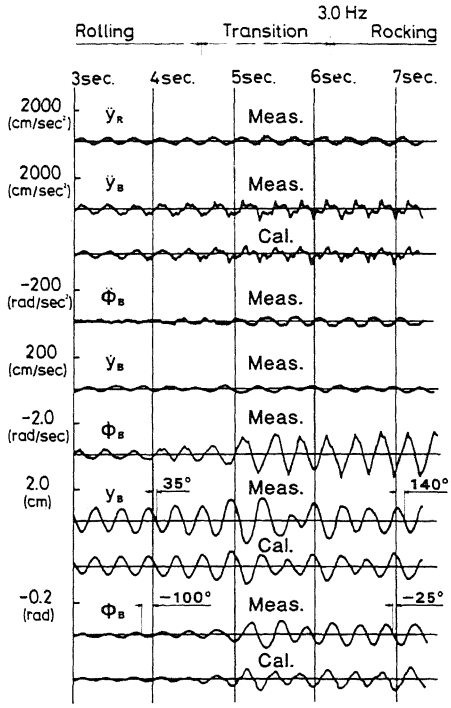

Fig. 10

Interrelation between Rocking and Derailment in Running Test

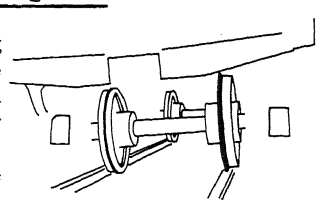

Fig. 11

The track excitations with the stable rocking for the standing vehicle sometimes entail the derailment in the running condition in the test. In this test, the derailment occurs more frequently than the rocking for higher-than-1.5-Hz frequencies. But these derailments are very few even under the same conditions(in acceleration amplitude, excitation frequency, running speed and so on), and there is preferably no observable tendency. Although in this study, we have still a lot of problems to be solved to make clear conditions governing the rocking followed by derailment, the occurrence of derailment is presumably greatly influenced by the sensitive tread contact situations between wheel and rail, such as the tread shape, friction coefficient, their relative positions by the yawing of the car body and so forth, and experimental investigations are now being conducted by systematically examining videotaped pictures of the derailment phenomena. One example is given in Fig.11 showing that either side of wheel flanges climbs up and crosses the rail, leading to derailment. Theoretical analyses on the occurrence of derailment are also being performed by developing the equations of motion (1) into the ones in the large motion, considering the tread contact effects between rail and wheel.

CONCLUSION

In this study, some of the points concerning rocking motion are made clear. While the derailment phenomena still has a lot of problems to be clarified to establish the definite interrelations to overturning or rocking. The equations of motion incorporating certain wheel factors are now being developed and experimental verifications by systematic examinations of collected data are also in progress.

REFERENCES

1) Research Committee on Runnability of Train and Honshu-Shikoku Bridge Authority: Runnability of Train on Honshu-Shikoku Bridges, Final Report, March 1982(In Japanese).
2) Yasoshima, Y., Y. Matsumoto and T. Nishioka: Studies on the running stability of railway vehicles on suspension bridges, Journal of the Faculty of Engineering, the University of Tokyo (B), Vol. XXXVI, No. 1, 1981.
3) Carter, F. W.: On the Action of a Locomotive Driving Wheel, Proc. Roy. Soc. Series A, Vol.112 (1926), 151.
4) Chartet, A., Acad. Sci. 225 (1947),986.